Journal of Molecular Catalysis A: Chemical 349 (2011) 42–47

Contents lists available at SciVerse ScienceDirect

Journal of Molecular Catalysis A: Chemical

journal homepage: www.elsevier.com/locate/molcata

Synthesis, characterization and catalytic properties of sulfonic acid functionalized magnetic-poly(divinylbenzene-4-vinylpyridine) for esterification of propionic acid with methanol

Ali Kara*, Beyhan Erdem

Department of Chemistry, Faculty of Science and Arts, Uludag University, 16059 Bursa, Turkey

ARTICLE INFO

Article history:
Received 21 June 2011
Received in revised form 11 August 2011
Accepted 17 August 2011
Available online 22 August 2011

Keywords:
Magnetic polymer
Esterification
Polymer synthesis
Acid catalyst

ABSTRACT

The magnetic-poly(divinylbenzene-4-vinylpyridine) [m-poly(DVB-4VP)] microbeads (average diameter: 180–212 μm) were synthesized by copolymerizing of divinylbenzene (DVB) with 4-vinylpyridine (4VP) and by mixing this copolymer with Fe_3O_4 nanoparticles. The resultant material was characterized by N_2 adsorption/desorption, ESR, elemental analysis, scanning electron microscope (SEM) and swelling studies. After functionalized with sulfonic acid, m-poly(DVB-4VP-SO_3H) was characterized by FT-IR and TGA analysis. The results showed that both of Fe_3O_4 and –SO_3H are bonded to the polymer successfully. N_2 adsorption/desorption isotherms of synthesized samples had the hysteresis behaviour associated with mesoporous materials (pore diameter: 3.73 nm). Sulfonic acid functionalized mesoporous m-poly(DVB-4VP-SO_3H) has been demonstrated to have higher reactivity than commercially available solid acid catalysts for the conversion of propionic acid to methyl ester. The apparent activation energy was found to be 38.5 kJ mol^{-1} for m-poly(DVB-4VP-20%SO_3H). The catalyst showed negligible loss of activity after four repetitive cycles.

Published by Elsevier B.V.

1. Introduction

In recent times, the development of environmentally benign green and easily recyclable catalyst for the production of fine chemicals has been an area of growing interest. In this context, solid acid catalysts play prominent role in organic synthesis under heterogeneous reaction conditions [1]. Heterogeneously catalysed chemical reactions are dramatically influenced by the strength and number of acid sites as well as the morphology of the support (surface area, pore size, etc.) [2]. Furthermore, functionalizing the surface of polymeric materials with organic groups have been investigated because surface modification permits tailoring of the surface properties for numerous potential applications including catalysis, ion exchange, encapsulation of transition-metal complexes or semiconductor clusters, chemical sensing, and nanomaterial fabrication [3]. Especially polymeric adsorbents incorporated with dithiocarbamate [4,5], dithizone [6], vinyl pyridine [7], phenylenediamine [8,9], chitosan [10], vinyl imidazole [11,12], diethylenetriamine [13], N-methacryloylhistidine [14], poly(ethyleneimine) [15,16], salicylaldoxime [17], tannic acid [18] and vinyl triazole [19] have been used extensively.

Studies on the preparation of various magnetic polymer microspheres have attracted more and more attention because magnetic separations are relatively rapid and easy, requiring simple equipment as compared to centrifugal separation [20]. Especially, Fe_3O_4 ferrites magnetic nanoparticles have been rising as a significant useful material due to their specific properties such as superparamagnetic, non toxic and small size, etc. [21]. The magnetic character implies that they respond to a magnet, making sampling and collection easier applications. Magnetic beads are commonly manufactured from polymers since they have a variety of surface functional groups which can be tailored to use in specific applications. For example, many polymeric magnetic are used in the removal of Cr(VI) ions [22–25]. In addition, they would find their applications in catalysts, medicines, sensors, and so on [26–33].

In this work we describe the preparation of a sulfonic acid functionalized m-poly(DVB-4VP) obtained by free radical polymerization technique in which the ferroferric oxide (Fe_3O_4) superparamagnetic nanoparticles was incorporated during the synthesis and its characterization in detail to obtain information about its structural, morphological and magnetic properties. So far as we know, no detailed investigation on the preparation of such a magnetic polymer material has been reported in the literature. And then its catalytic performance was tested for the esterification of propionic acid with methanol and compared with the traditional catalysts such as Amberlyst and

* Corresponding author. Tel.: +90 2242941733; fax: +90 2242941899.
E-mail address: akara@uludag.edu.tr (A. Kara).

1381-1169/$ – see front matter. Published by Elsevier B.V.
doi:10.1016/j.molcata.2011.08.016

Dowex which are the best known catalysts for the esterification reactions.

2. Experimental

2.1. Materials

Divinilbenzene (DVB) was obtained from Merck (Darmstadt, Germany), and inhibitor was rendered by washing with NaOH solution (3%, w/w) prior to use. 4-Vinylpyridine (4VP) was obtained from Fluka (Steinheim, Germany). 2,2′-Azobisisobutyronitrile (AIBN) was obtained from Merck (Darmstadt, Germany). Poly(vinyl alcohol) (PVAL; Mw: 72.000, 98% hydrolyzed) was supplied from Merck (Darmstadt, Germany). Magnetite nanopowder (Fe_3O_4; diameter 20–30 nm) was obtained from Aldrich (Steinheim, Germany). All other reagents were of analytical grade and were used without further purification.

2.2. Preparation of m-poly(DVB-4VP-SO_3H) microbeads

DVB and 4VP were copolymerized in suspension by using AIBN and poly(vinyl alcohol) as the initiator and the stabilizer, respectively. Toluene was included in the polymerization recipe as the diluent (as a pore former). A typical preparation procedure was exemplified below: Continuous medium was prepared by dissolving poly(vinyl alcohol) (200 mg) in the purified water (50 mL). For the preparation of dispersion phase, DVB (2.9 mL; 20 mmol) magnetite Fe_3O_4 nanopowder (0.5 g) and toluene (10 mL) were stirred for 10 min at room temperature. Then, 4VP (8.6 mL; 80 mmol) and AIBN (100 mg) were dissolved in the homogeneous organic phase. The organic phase was dispersed in the aqueous medium by stirring the mixture magnetically (500 rpm), in a sealed-cylindrical pyrex polymerization reactor. The reactor content was heated to polymerization temperature (i.e., 65 °C) within 4 h and the polymerization was conducted for 2 h with a 600 rpm stirring rate at 80 °C. The final microbeads were extensively washed with ethanol and water to remove any unreacted monomer or diluent and then dried at 50 °C in a vacuum oven. The microbeads then were sieved to different sizes. An inspection with a microscope showed that almost all the microbeads were perfectly spherical. Table 1 shows recipe and polymerization conditions for preparation of the mesoporous m-poly(DVB-4VP) microbeads. The m-poly(DVB-4VP-SO_3H) catalysts were prepared by mixing of different percentages of H_2SO_4 solution (10% and 20%, respectively) with m-poly(DVB-4VP) polymer at 298 K in a sealed cylindrical pyrex reactor for 2 h. The solid was filtered and vacuum dried at 343 K overnight and stored in the glove box for characterizations.

2.3. Characterization of m-poly(DVB-4VP) and its sulfate microbeads

The porosity of the microbeads was measured by N_2 gas adsorption/desorption isotherm technique (Quantachrome Corporation, Poremaster 60, USA). The specific surface area of the beads in a dry state was determined by a multipoint Brunauer–Emmett–Teller (BET) and pore volumes and average pore diameter for the beads were determined by the BJH (Barrett, Joyner, Halenda) model. In addition, the average size and size distribution of the beads were determined by screen analysis performed using standard sieves (Model AS200, Retsch Gmb & Co., KG, Haan, Germany).

The surface structures of the beads were visualized and examined by scanning electron microscopy (SEM, CARL ZEISS EVO 40, UK).

In order to evaluate the degrees of (4VP) incorporation and to test whether sulfur enters to the polymeric structure, m-poly(DVB-4VP) (Sample I), and m-poly(DVB-4VP-SO_3H) having 10 and 20 percentages of H_2SO_4 (Samples II and III) beads were subjected to elemental analysis with LECO CHNS-932 model elemental analyzer.

The presence of magnetite nano-powders in the beads was investigated with an electron spin resonance (ESR) spectrophotometer (EL 9, Varian, USA).

FTIR measurements were performed on a Thermo Nicolet 6700 series FTIR spectrometer in normal transmission mode with a KBr detector over the range 4000–400 cm^{-1} at a resolution 8 cm^{-1} averaged over 32 scans.

Thermal stabilities of the m-poly(DVB-4VP) and its sulfonic acid functionalized forms were examined by TG analyses with SII-EXSTAR TG/DTA 6200. The samples (~5–10 mg) were heated from room temperature to 800 °C under dried-air atmosphere at a scanning rate of 10 °C/min.

The acid exchange capacities of the m-poly(DVB-4VP-SO_3H) prepared with 10% and 20% H_2SO_4 were measured by means of titration, using sodium chloride as exchange agent. In a typical experiment, 0.05 g of solid was added to 10 g of aqueous solution of sodium chloride (2 M). The resulting suspension was allowed to equilibrate and thereafter titrated potentiometrically by drop-wise addition of 0.01 M NaOH (aq) [34].

2.4. Catalytic conditions

The esterification of propionic acid with methanol was carried out in a glass flask placed in the shaking water bath the temperature of which was controlled within ±0.1 °C. Stoichiometric ratio of propionic acid to methanol was (1:1) in the experiments performed at 333 K. 1,4-Dioxane was used as solvent in the all experiments. In a typical run, catalyst (about 0.5 g), methanol and dioxane of known amount were charged in to the reactor and preheated to the reaction temperature and the esterification was commenced by injecting preheated propionic acid in to the mixture. This was considered as the zero time for a run. The total liquid volume was 100 cm^3. Samples were withdrawn and the amount of unreacted acid was analysed by titration with 0.1 M sodium hydroxide.

2.5. Effect of temperature

The effect of temperature is very important for a heterogeneously catalysed reaction as this information is useful in calculating the apparent activation energy. Moreover, the intrinsic rate constants are strong functions of temperatures [35]. To calculate the apparent activation energy the reaction temperature was changed from 318 K to 348 K by keeping the same experimental conditions such as (1:1) mole ratio, 0.5 g catalyst loading, and by using 1,4-dioxane as solvent.

2.6. Reuse of catalyst

At the end of the reaction, catalyst was separated from the reaction mixture in the presence of external magnetic fields and was thoroughly washed with deionised water several times. After the reaction the catalyst was activated in the potentially containing 20% H_2SO_4 solution for 2 h and dried under vacuum at 333 K and then used as catalyst for recycling experiments. This whole process has been continued four times.

3. Results and discussion

The suspension polymerization procedure provided cross-linked mesoporous m-poly(DVB-4VP) microbeads in the spherical form of 106–212 μm in diameter. The N_2 adsorption/desorption isotherm for the m-poly(DVB-4VP) and the calculated pore size distributions are plotted in Fig. 1. The BET surface area (S_{BET}), pore volume (V_P) and pore size are given in Table 2. The sample

Table 1
Recipe and polymerization conditions for preparation of the mesoporous m-poly(DVB-4VP) microbeads.

Polymerization conditions	Aqueous dispersion phase	Organic phase
Reactor volume: 100 mL Stirring rate: 600 rpm Temperature and time: 65 °C (4 h), 80 °C (2 h)	Distilled water: 50 mL PVAL: 200 mg	DVB: 2.9 mL 4VP: 8.6 mL Toluene: 10 mL AIBN: 100 mg Fe_3O_4: 0.5 g

Table 2
BET surface area, pore volume and pore size of m-poly (DVB-4VP).

Sample	BET surface area ($m^2\ g^{-1}$)	Pore volume ($cm^3\ g^{-1}$)	Pore size (Å)
m-poly(DVB-4VP)	23.24	0.1020	37.31

gave a type IV isotherm with a deep inflection between relative pressure $P/P_o = 0.4$ and 0.9, a characteristic of capillary condensation, indicating the uniformity of the mesopore-size distribution [36–38]. This indicated that the magnetic beads contained mainly mesopores.

The equilibrium swelling ratio for the mesoporous m-poly(DVB-4VP) microbeads is 62% in water. It should be also noted that these microbeads are strong enough due to highly cross-linked structure therefore they are suitable for column applications.

The surface morphology and bulk structures of the m-poly(DVB-4VP) microbeads were visualized by SEM which are presented in Fig. 2. All the beads have a spherical form and rough surface. In the SEM photograph of the bulk structure, a large quantity of well-distributed pores could be observed and they have netlike structure. The mesoporous m-poly(DVB-4VP) microbeads prepared in this study had this characteristics and this property increases the specific surface area, the binding capacity of microbeads, as well as the mass transfer rate of binding.

The m-poly(DVB-4VP) microbeads were synthesized by copolymerizing DVB with 4VP at a 1:4 molar ratio with Fe_3O_4 in the presence of the initiator AIBN. To evaluate the degree of 4VP incorporation into the mesoporous m-poly(DVB-4VP) microbeads, elemental analysis of the synthesized mesoporous m-poly(DVB-4VP) microbeads was performed (Table 3). The incorporation of the 4VP was found to be 872.9 μmol/g polymer from the nitrogen stoichiometry. This is clear evidence indicating that SO_3H groups are located in the polymer, thus being accessible and useful for adsorption and catalytic reaction processes. According to the elemental analyses results *C*/*N* ratio do not changed, so there is not any degradation doubt.

Magnetic characteristics of magnetic materials are related to their type generally, while those of magnetic materials are usually related to the content of magnetic component inside. So, Fe_3O_4 content is very important to the magnetic responsibility of magnetic materials. In general, the higher Fe_3O_4 content shows the stronger magnetic responsibility [33]. For this reason, the average Fe_3O_4 content of the mesoporous m-poly(DVB-4VP) microbeads was determined by density analysis. The hydrated density of the mesoporous m-poly(DVB-4VP) microbeads measured at 25 °C was 1.53 g/mL. By the same procedure, the density of Fe_3O_4 particles was found to be 4.94 g/mL at 25 °C. The density of non-magnetic poly(DVB-4VP) microbeads measured at 25 °C was 1.05 g/mL. The magnetic particles volume fraction in the

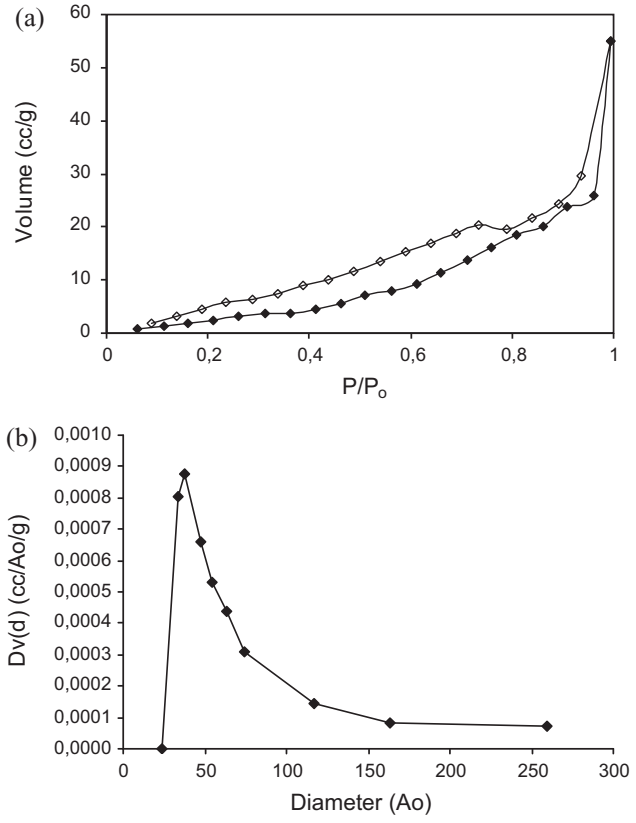

Fig. 1. (A) Adsorption/desorption isotherms of nitrogen at 77.40 K and (B) pore size distribution obtained by Dv(d) according to average pore diameter for the m-poly (DVB-4VP).

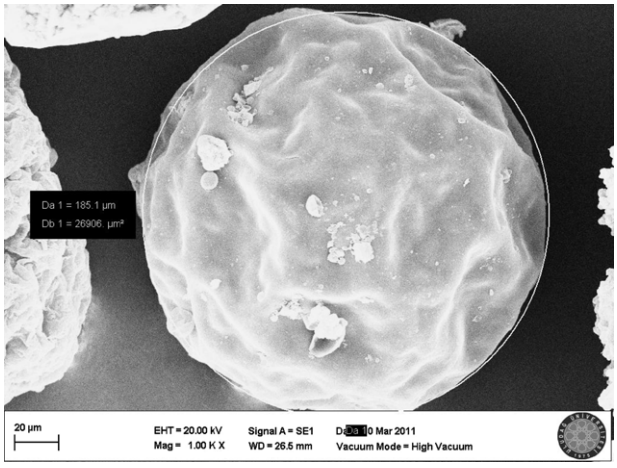

Fig. 2. SEM photograph of the m-poly(DVB-4VP) microbeads.

Table 3
Elemental analysis of the mesoporous m-poly(DVB-4VP) microbeads.

Sample	C (%)	H (%)	N (%)	S (%)
(I) m-poly(DVB-4VP)	68.58	6.56	8.16	–
Theoretical values	82.91	6.91	10.18	–
(II) m-poly(DVB-4VP-10%SO_3H)	41.68	5.03	5.06	13.82
(III) m-poly(DVB-4VP-20%SO_3H)	34.30	5.20	4.19	15.62

mesoporous m-poly(DVB-4VP) microbeads can be calculated from the following equation derived from the mass balance:

$$\phi = \frac{\rho_C - \rho_M}{\rho_C - \rho_A} \quad (1)$$

where ρ_A, ρ_C and ρ_M are the densities of non-magnetic poly(DVB-4VP) microbeads, Fe_3O_4 nanopowder, and the mesoporous m-poly(DVB-4VP) microbeads, respectively. Thus, with the density data mentioned above, the mesoporous m-poly(DVB-4VP) microbeads gel volume fraction in the magnetic beads was estimated to be 84.3%. Therefore, the average Fe_3O_4 content of the resulting mesoporous m-poly(DVB-4VP) microbeads was 12.3%. The presence of magnetite nanopowder in the polymer structure was also confirmed by the ESR. The intensity of the magnetite peak against magnetic field (Gauss) is shown in Fig. 3. A peak of magnetite was detected in the ESR spectrum. It should be noted that the non-magnetic beads cannot be magnetized under this condition. It reflects response ability of magnetic materials to the change of external magnetic field firstly and it characterizes the ability of magnetic materials to keep magnetic field strength when the external magnetic field is removed. In order to show the magnetic stability, the mesoporous m-poly(DVB-4VP) microbeads were kept in distilled water and ambient air for 3 months, and the same ESR spectrum was obtained. With the goal of testing the mechanical stability of the mesoporous m-poly(DVB-4VP) microbeads, a bead sample was treated in a ball mill for 12 h. SEM photographs show that a zero percentage of the sample was broken. The *g* factor given in Fig. 3 can be considered as quantity characteristic of the molecules in which the unpaired electrons are located, and it is calculated from Eq. (2). The measurement of the *g* factor for an unknown signal can be a valuable aid in the identification of a signal. In the literature, the *g* factor for Fe^{3+} is determined within the range of 1.4–3.1 for low spin and 2.0–9.7 for high spin complexes [33]. The *g* factor was found to be 2.43 for the mesoporous m-poly(DVB-4VP) microbeads.

$$g = \frac{h\vartheta}{\beta H_r} \quad (2)$$

Here, h is the Planck constant (6.626×10^{-27} erg s^{-1}); β is Universal constant (9.274×10^{-21} erg G^{-1}); ϑ is frequency (9.707×10^{9} Hz) and H_r is resonance of magnetic field (G).

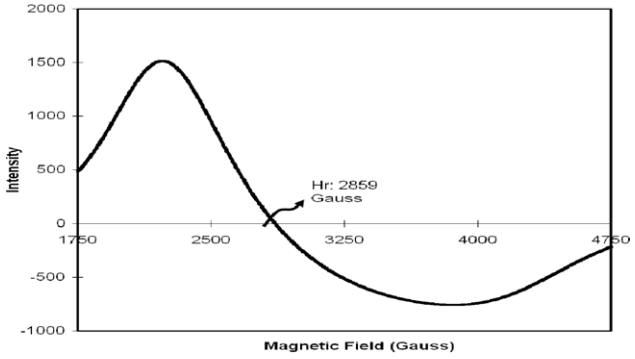

Fig. 3. ESR spectrum of the m-poly(DVB-4VP) microbeads.

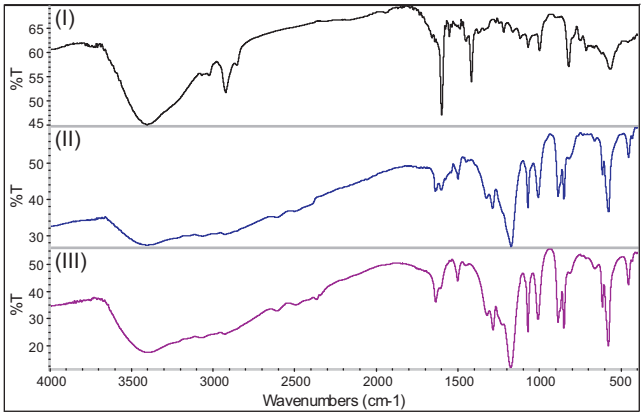

Fig. 4. FT-IR spectra of m-poly(DVB-4VP) (I) and its 10% and 20% sulfonic acid functionalized forms (II and III), respectively.

Fig. 4 shows the FT-IR spectra of m-poly(DVB-4VP) (I) and its sulfonic acid functionalized forms with 10% H_2SO_4 (II) and 20% H_2SO_4 (III), respectively. The absorption bands around 1600, 1550 and 1500 cm^{-1} are assigned to the characteristic vibration of pyridine ring. The absorption bands around 1068 and 960 cm^{-1} are assigned to the in-plane and out-of-plane rings C–H bending [39]. The introduction of Fe_3O_4 to the poly(DVB-4VP) was confirmed by the band at 585 cm^{-1} assigned to the Fe-O absorption band (Samples I–III) [40,41]. Compared to m-poly(DVB-4VP), the distinguished features of m-poly(DVB-4VP-SO_3H) were the presence of new absorption bands around 1100 cm^{-1} and 610 cm^{-1} which are attributed to the stretching and bending for S–O vibrations [42]. The intensities of these peaks also increase in parallel with the increase in the percentage of H_2SO_4 in the blends [43].

Fig. 5 shows the TGA curves of m-poly(DVB-4VP) (Sample I) and m-poly(DVB-4VP-SO_3H) (Samples II and III). In these curves, three main reaction stages are observed. For Sample I, the exponential weight decay until 100 °C can be attributed to absorbed humidity. While the weight loss at 300–370 °C region may be attributed to degradation of DVB chain, the 480–600 °C region is

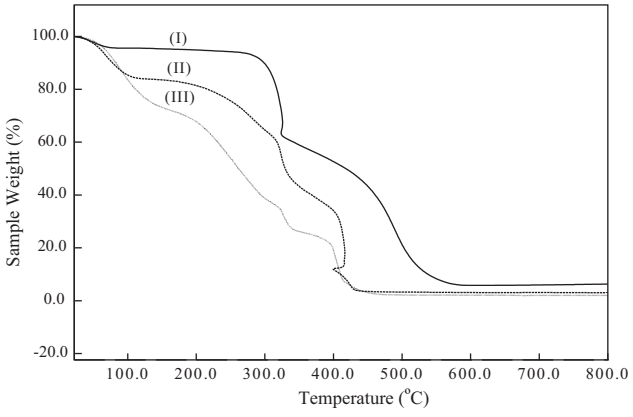

Fig. 5. TGA analysis of m-poly(DVB-4VP) (I) and its 10% and 20% sulfonic acid functionalized forms (II and III), respectively.

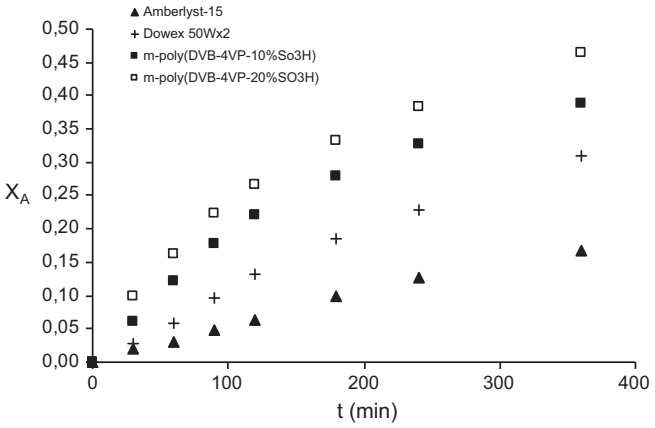

Fig. 6. Catalytic results for the esterification of propionic acid with methanol (60 °C; PA:MeOH = 1:1; catalyst, 0.5% Amberlyst-15 (▲), 0.5% Dowex 50WX2 (+), 0.5% m-poly(DVB-4VP-10%SO_3H) (■), and 0.5% m-poly(DVB-4VP-20%SO_3H) (□)).

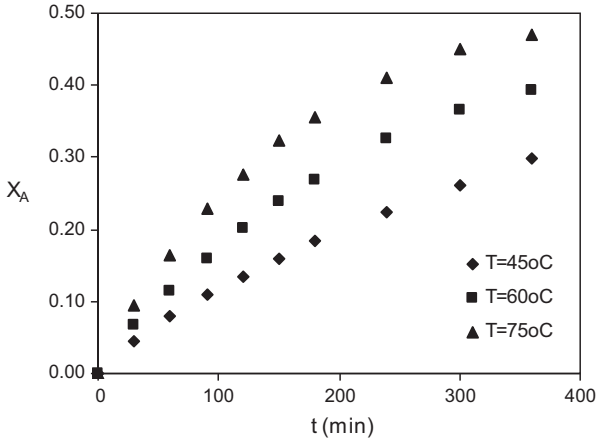

Fig. 7. Effect of temperature on the conversion of propionic acid over m-poly(DVB-4VP-20%SO_3H) catalyst.

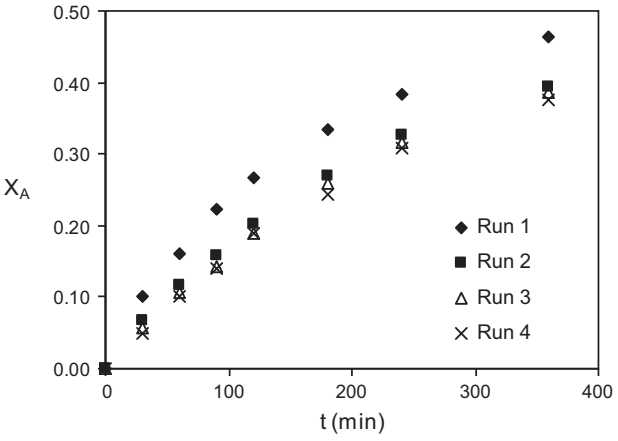

Fig. 8. Kinetic plots of recycling test of m-poly(DVB-4VP-20%SO_3H) in the esterification reaction of methanol with propionic acid.

mainly attributed to thermo-oxidative degradation of PVP polymer chain [44]. The m-poly(DVB-4VP-SO_3H) (Samples II and III) illustrate that there is weight decay up to 160 °C because of absorbed humidity similar to pristine polymer. If all sulfur elements in the catalyst are assumed as –SO_3H groups, weight change from 370 °C to 500 °C can be attributed to self-condensation of –SO_3H.

To provide a comparison basis for the acid catalysts, the esterification reaction was also performed with two commercial acidic resins, Amberlyst-15 and Dowex 50WX2. Shown in Fig. 6 are the results for the reaction studies performed at 60 °C with a methanol to propionic acid ratio of 1:1 by weight. Experiments were carried out under identical conditions except for the type of catalyst. The figure gives the propionic acid conversion as a function of reaction time. A catalyst concentration of 0.5 wt% was used for all of the catalysts. Between the sulfonic acid functionalized m-poly(DVB-4VP-SO_3H) catalysts, m-poly(DVB-4VP-20%SO_3H) gave the higher catalytic activity than that of m-poly(DVB-4VP-10%SO_3H) with propionic acid conversions of 47% and 39%, respectively, after 6 h. The equilibrium conversion of propionic acid was the same in all experiments as expected. The highest activity with m-poly(DVB-4VP-20%SO_3H) was consistent with the material having the largest number of active sites (7.43 mequiv./g sample) among the other acid catalysts, i.e., m-poly(DVB-4VP-10%SO_3H) (6.70 mequiv./g sample), Dowex 50WX2 (4.8 mequiv.meq/g) and Amberlyst-15 (4.7 mequiv./g). Results suggested that our mesoporous m-poly(DVB-4VP-SO_3H) material is a superior catalyst for the production of methyl propionate over the existing catalysts known in the literature.

In order to evaluate the m-poly(DVB-4VP-20%SO_3H) catalyst thermodynamically, model esterification reaction was performed at different temperatures from 318 to 348 K by keeping the same experimental conditions such as (1:1) mole ratio, 0.5 g catalyst loading, and by using 1,4-dioxane as solvent. Reaction rate constants (k) were calculated according to pseudo-homogeneous second order rate equation [45,46]:

$$\ln \frac{X_{PA,e} - (2X_{PA,e} - 1)X_{PA}}{X_{PA,e} - X_{PA}} = 2k \left(\frac{1}{X_{PA,e}} - 1 \right) C_{PA,0} t \quad (3)$$

where X_{PA}, fractional conversion of propionic acid,

$$X_{PA} = \frac{C_{PA,0} - C_{PA}}{C_{PA,0}} \quad (4)$$

As the reaction temperature increased, the reaction kinetics was faster for m-poly(DVB-4VP-20%SO_3H) (Fig. 7), but equilibrium conversion was nearly the same in the range of temperatures studied in this work.

$$\ln k = \ln A - \frac{E_A}{R} \left(\frac{1}{T} \right) \quad (5)$$

The activation energy obtained for 20%-SO_3H-loaded m-poly(DVB-4VP) is 38.5 kJ mol^{-1}, which is very similar and close to the value found in the literature [43].

Regeneration is likely to be a key factor in the improvement of process economics. For this reason, the regeneration property of m-poly(DVB-4VP-SO_3H) beads is worthy of study. At this stage we envisioned that the only manner in which the m-poly(DVB-4VP-SO_3H) could be restored to its original activity would be to oxidise it back to its beginning form. To determine the reusability of m-poly(DVB-4VP-SO_3H), the consecutive esterification reactions were repeated 4 times with the same catalyst. Catalytic activity and conversion for each cycle are given in Fig. 8. Catalyst activity decreased 20% after the first cycle because of the lack of catalyst mass and the rate of conversion of lactic acid was maintained almost the same during the next three cycles. Thus the mesoporous m-poly(DVB-4VP-SO_3H) material described herein has great potential to be a stable and highly active recyclable solid acid catalyst.

4. Conclusions

We have successfully prepared the sulfonic acid functionalized magnetic poly(DVB-4VP) by incorporating Fe_3O_4 nanoparticles and

H_2SO_4 to the copolymer of divinylbenzene with 4-vinylpyridine. The result of field dependence of magnetization was consistent with the microscopic observation. Tuning the acidity of the active site can enhance the performance of the mesoporous materials. Increasing the acidity of sulfonic acid group was found to improve significantly the activity of the catalyst for the propionic acid esterification reaction. This work demonstrates the potential of mesoporous m-poly(DVB-4VP-SO_3H) materials for rational design of heterogeneous catalysts. Moreover, this mesoporous solid acid catalyst has been recycled four times with negligible loss of activity, suggesting high chemical stability and reusability of the m-poly(DVB-4VP-SO_3H) framework.

Acknowledgement

This work was supported by the Research Foundation of Uludag University (Project No.: UAP(F)-2011/35).

References

[1] R.I. Kureshy, I. Ahmad, K. Pathak, N.H. Khan, S.H.R. Abdi, R.V. Jasra, Catal. Commun. 10 (2009) 572–575.
[2] B. Sow, S. Hamoudi, M.H. Zahedi-Naki, S. Kaliaguine, Micropor. Mesopor. Mater. 79 (2005) 129–136.
[3] M.H. Lim, A. Stein, Chem. Mater. 11 (1999) 3285–3295.
[4] R. Say, E. Birlik, A. Denizli, A. Ersöz, Appl. Clay Sci. 31 (2006) 298–305.
[5] E. Pişkin, K. Kesenci, N. Şatıroğlu, Ö. Genç, J. Appl. Polym. Sci. 59 (1996) 109–117.
[6] B. Salih, A. Denizli, C. Kavaklı, R. Say, E. Pişkin, Talanta 46 (1998) 1205–1213.
[7] A. Duran, M. Soylak, S.A. Tuncel, J. Hazard. Mater. 155 (2008) 114–120.
[8] X.G. Li, X.L. Ma, J. Sun, M.R. Huang, Langmuir 25 (2009) 1675–1684.
[9] Q.F. Lu, M.R. Huang, X.G. Li, Chem. Eur. J. 13 (2007) 6009–6018.
[10] G.J. Copello, F. Varela, R.M. Vivot, L.E. Diaz, Bioresour. Technol. 99 (2008) 6538–6544.
[11] A. Kara, L. Uzun, N. Beşirli, A. Denizli, J. Hazard. Mater. 106B (2004) 93–99.
[12] N. Fontanals, R.M. Marce, M. Galia, F. Boorrull, J. Macromol. Sci. Pure Appl. Chem. A42 (2004) 2019–2025.
[13] C. Liu, R. Bai, L. Hong, J. Colloids Interf. Sci. 303 (2006) 99–108.
[14] R. Say, B. Garipcan, S. Emir, S. Patır, A. Denizli, Macromol. Mater. Eng. 287 (2002) 539–545.
[15] G. Bayramoğlu, M.Y. Arıca, Sep. Purif. Technol. 45 (2005) 192–199.
[16] R. Say, A. Tuncel, A. Denizli, J. Appl. Polym. Sci. 83 (2002) 2467–2473.
[17] K.A.K. Ebraheem, S.T. Hamdi, React. Funct. Polym. 34 (1997) 5–10.
[18] A. Üçer, A. Uyanık, Ş.F. Aygün, Sep. Purif. Technol. 47 (2006) 113–118.
[19] A. Kara, J. Appl. Polym. Sci. 114 (2009) 948–955.
[20] S. Wei, Y. Zhu, Y. Zhang, J. Xu, React. Funct. Polym. 66 (2006) 1272–1277.
[21] D.T.K. Dung, T.H. Hai, L.H. Phuc, B.D. Long, L.K. Vinh, P.N. Truc, J. Phys. Conf. Ser. 187 (2009) 012036.
[22] G. Huang, H. Zhang, J.X. Shi, T.A.G. Langrish, Ind. Eng. Chem. Res. 48 (2009) 2646–2651.
[23] G. Bayramoglu, M.Y. Arıca, Chem. Eng. J. 139 (2008) 20–28.
[24] J. Hu, G.H. Chen, M.C.L. Irene, Water Res. 39 (2005) 4528–4536.
[25] H. Li, Z. Li, T. Liu, X. Xiao, Z. Peng, L. Deng, Bioresour. Technol. 99 (2008) 6271–6279.
[26] Y.G. Zhao, H.Y. Shen, S.D. Pan, M.Q. Hu, J. Hazard. Mater. 182 (2010) 295–302.
[27] M.E. Çorman, N. Öztürk, N. Tüzmen, S. Akgöl, A. Denizli, Biochem. Eng. J. 49 (2010) 159–164.
[28] I. Safarik, M. Safarikova, Hacettepe J. Biol. Chem. 38 (2010) 1–7.
[29] E. Mosiniewicz-Szablewska, M. Safarikova, I. Safarik, J. Nanosci. Nanotechnol. 10 (2010) 2531–2536.
[30] I. Safarik, M. Safarikova, Chem. Pap. 63 (2009) 497–505.
[31] H. Yavuz, A. Denizli, H. Gungunes, M. Safarikova, I. Safarik, Sep. Purif. Technol. 52 (2006) 253–260.
[32] D. Müller-Schhulte, T. Schmitz-Rode, J. Magn. Magn. Mater. 302 (2006) 267–271.
[33] S. Şenel, L. Uzun, A. Kara, A. Denizli, J. Macromol. Sci. Pure Appl. Chem. A45 (2008) 635–642.
[34] D. Margolese, J.A. Melero, S.C. Christiansen, B.F. Chmelka, G.D. Stucky, Chem. Mater. 12 (2000) 2448–2459.
[35] B. Erdem, A. İzci, Z. Phys. Chem. 224 (2010) 781–793.
[36] G. Duan, C. Zhang, A. Li, X. Yang, L. Lu, X. Wang, Nanoscale Res. Lett. 3 (2008) 118–122.
[37] R.B. Restani, V.G. Correia, V.D.B. Bonifácio, A.A. Ricardo, J. Supercrit. Fluids 55 (2010) 333–339.
[38] L.J. Fu, T. Zhang, Q. Cao, H.P. Zhang, Y.P. Wu, Electrochem. Commun. 9 (2007) 2140–2144.
[39] K.H. Wu, Y.R. Wang, W.H. Hwu, Polym. Degrad. Stab. 79 (2003) 195–200.
[40] B. Mu, T. Wang, Z. Wu, H. Shi, D. Xue, P. Liu, Colloids Surf. A Physicochem. Eng. Aspects 375 (2011) 163–168.
[41] K. Can, M. Ozmen, M. Ersoz, Colloids Surf. B Biointerf. 71 (2009) 154–159.
[42] A. Stoch, J. Stoch, J. Gurbiel, M. Cichocinska, M. Mikolajezyk, M. Timler, J. Mol. Struct. 596 (2001) 201–206.
[43] B. Erdem, A. Kara, React. Funct. Polym. 71 (2011) 219–224.
[44] X.G. Li, React. Funct. Polym. 42 (1999) 53–58.
[45] B. Erdem, M. Cebe, Korean J. Chem. Eng. 23 (6) (2006) 896–901.
[46] A. İzci, F. Bodur, React. Funct. Polym. 67 (2007) 1458–1464.